Biochem. J. (1976) **155**, 279–295
Printed in Great Britain

The Circular Dichroism of Ribosomal Ribonucleic Acids

By ROBERT A. COX, WILLIAM HIRST, ELIZABETH GODWIN and IVAN KAISER*
National Institute for Medical Research, Mill Hill, London NW7 1AA, U.K.

(*Received* 10 *October* 1975)

1. The c.d. (circular dichroism) of *Drosophila melanogaster* rRNA (42% G+C) and of G+C-rich fragments (78% G+C) obtained by partial hydrolysis of rabbit L-rRNA (the largest RNA species isolated from the large subribosomal particle) were measured and found to differ substantially. 2. To interpret these spectra a relation between c.d. of bihelical RNA and % G+C was derived, namely $\Delta\varepsilon_{f_G} = af_G^2 + bf_G + c$, where $\Delta\varepsilon_{f_G}$ is the c.d. of RNA characterized by a mole fraction, f_G, of guanine nucleotides and a, b and c are constants. 3. A frame of reference was established by studying the c.d. of a range of rRNA species, including S-rRNA (the RNA species isolated from the smaller subribosomal particle) and L-rRNA of *Escherichia coli*. 4. It was found for the rRNA species studied that 0.60 ± 0.05 of residues appear to form bihelical secondary structure. 5. A higher helical content, 0.66 ± 0.05, was found for the G+C-rich fragment of L-rRNA. The difference in the c.d. of rabbit L-rRNA and of *D. melanogaster* rRNA is attributable to the dependence of c.d. of the bihelical parts on % G+C. 6. The minimum in c.d. at 295nm increases with increasing % G+C. The c.d. of rRNA was compared with that of the parent subparticle in this region of the spectrum, where high precision may be attained.

A feature of L-rRNA† of certain eukaryotes is that guanine and cytosine residues are unevenly distributed throughout the molecule (see, e.g., Cox *et al.*, 1973*a*; Godwin *et al.*, 1974). Partial nuclease hydrolysis of rabbit L-rRNA (67% G+C) yielded fragments of approx. 0.4×10^6 daltons that were rich in G+C (approx. 78%). Electron microscopy has revealed the configuration of particular regions of L-rRNA and pre-rRNA where secondary structure withstands the denaturing conditions used in the preparation of the samples (Wellauer & Dawid, 1973; Schibler *et al.*, 1975). There is direct evidence to show that these stable structures arise from regions rich in G+C residues (Godwin *et al.*, 1974; Schibler *et al.*, 1975). These regions of stable secondary structure appear to be characteristic of vertebrate L-rRNA and pre-rRNA.

In contrast, *Drosophila melanogaster* L-rRNA (42% G+C) has tracts rich in A+U residues (approx. 25–30% G+C), as shown by Godwin *et al.* (1974). Although the nucleotide composition of intact L-rRNA from different species ranges from 35% to 67% G+C (Lava-Sanchez *et al.*, 1972), the range is even greater (25–78% G+C) when fragments of L-rRNA are compared. The question arises of what kinds of secondary structure are generated by these different primary sequences.

The c.d. spectrum of an RNA species reflects its secondary structure, there being contributions from both the bihelical and the single-stranded parts (see, e.g., Blum *et al.*, 1972). The c.d. spectrum of fragments of rabbit L-rRNA (approx. 78% G+C) differs appreciably from that of L-rRNA (approx. 42% G+C) of *D. melanogaster* ($\Delta\varepsilon_{260} = 5.0 \pm 0.3$ and 7.4 ± 0.3 $l \cdot mol^{-1} \cdot cm^{-1}$ respectively; $\Delta\varepsilon_{280} = 1.3 \pm 0.2$ and 2.7 ± 0.2 $l \cdot mol^{-1} \cdot cm^{-1}$ respectively; $\Delta\varepsilon_{295} = 0.66 \pm 0.02$ and -0.16 ± 0.02 $l \cdot mol^{-1} \cdot cm^{-1}$ respectively) to an extent that needs explanation.

Previous work on the c.d. of rRNA (Yang & Samejima, 1969; Gratzer & Richards, 1971) does not provide a basis for the interpretation of the difference of the above-mentioned spectra. To establish a frame of reference, we examined the c.d. of several other rRNA species (S-rRNA and L-rRNA of *Escherichia coli* and S-rRNA and L-rRNA of rabbit). The c.d. of S-rRNA of *E. coli* is an important reference compound for c.d. studies because its primary structure is largely known and because a scheme for secondary structure based on its nucleotide sequence has been proposed (Ehresmann *et al.*, 1972). Few physical measurements yielding quantitative information

* Permanent address: Division of Biochemistry, University of Wyoming, Laramie, WY 82071, U.S.A.

† Abbreviations: L-rRNA, the largest RNA species isolated from the large subribosomal particle; S-rRNA, the RNA species isolated from the smaller subribosomal particle; L-sRS and S-sRS, the large and small subribosomal particles respectively; c.d., circular dichroism; f_{GC}, the mole fraction of G+C residues in the bihelical segments of rRNA; hypochromism is defined as the difference in extinction of RNA under specified conditions compared with the extinction measured at 95°C in a solvent where bihelical structure is absent and the extinction rises by no more than 1% for a further 10°C rise in temperature.

about the number of base-pairs etc. of *E. coli* S-rRNA have been made; instead, results obtained from studies of an unfractionated mixture of S-rRNA and L-rRNA (1:2, w/w) have been extrapolated to S-rRNA, even though it is clearly the minor component.

The c.d. spectra were analysed by a method based on that described by Blum *et al.* (1972) for tRNA. A consistent picture for the secondary structure of rRNA emerged. In each case 55–65% of residues appear to form bihelical secondary structure and a further 20% of residues appear to 'stack' in single-stranded regions. A slightly higher 'helical content' (0.66 ± 0.05) was found for G+C-rich fragments of rabbit L-rRNA. Hence the high stability of the G+C-rich regions does not arise from a substantially higher bihelical content.

It was noted that the minimum in c.d. at 295nm became more pronounced with increasing % G+C. More precise measurements of c.d. at this wavelength may be achieved by increasing the rRNA concentration, and this led us to re-examine and again compare the c.d. of rRNA and its parent ribosome particularly in this region.

Theoretical

Blum *et al.* (1972) showed that the c.d. of tRNA may be calculated from eqn. (1):

$$\Delta\varepsilon_{obs.} = \Delta\varepsilon_{bh} + \Delta\varepsilon_{ss} + T \qquad (1)$$

where $\Delta\varepsilon_{obs.}$ is the observed c.d., $\Delta\varepsilon_{bh}$ is the contribution of residues in bihelical parts, $\Delta\varepsilon_{ss}$ is the contribution to c.d. of the single-stranded parts and T is the contribution from tertiary structure. Tertiary structure may contribute to c.d. in at least two ways: (i) the formation of base-pairs may alter the proportion of residues that 'stack' in single-stranded regions of a hairpin loop, and (ii) hairpin loops may interact further, as in tRNA, to form a clearly defined structure. T includes the contributions to c.d. of both effects (i) and (ii). The assumptions made and the approximations and relations used in this analysis are given below.

Calculation of the c.d. of the bihelical parts

(1) The c.d. of a particular base-pair in a bihelical region or of a residue in a single-stranded region is dependent mainly on its nearest neighbour (see Blum *et al.*, 1972).

(2) The c.d. of the bihelical parts arises from the contributions of ten possible first-neighbour interactions between base-pairs (Blum *et al.*, 1972) [see also the Appendix (Cox & Hirst, 1976)]. Hence:

$$\Delta\varepsilon(\lambda) = 1/N \sum_{i=1}^{10} N_i C_i(\lambda) \qquad (2)$$

where N is the number of base-pairs, N_i is the number of times each of the ten nearest-neighbour couples occurs, and $C_i(\lambda)$ is the contribution of couple i per mol of nucleotide residue to c.d.

(3) The frequency P_i with which the couple i occurs is the same as if the nucleotide sequence were random, i.e.:

$$P_i = N_i/N \qquad (3)$$

This assumption was tested for *E. coli* S-rRNA by comparing values of P_i calculated by means of eqn. (3) and values of N_i/N calculated from the model of primary sequence proposed by Ehresmann *et al.* (1972). The values given in Table 1 reveal that the two estimates differ at most by approx. 25%. The c.d. spectrum calculated by means of eqn. (2) by using the values of P_i obtained by means of eqn. (3) was scarcely distinguishable from the spectrum calculated from values of N_i/N obtained from primary sequence data. On this basis eqn. (3) is a valid approximation.

(4) Interactions between base-paired couples are the same in the bihelical parts of rRNA as in high polymers. The basis for this assumption is that c.d. depends on the precise conformation of the neighbouring base-pairs. The bihelical parts of rRNA that have been studied by X-ray methods appear to have a structure identical with that found for bihelical RNA (Arnott *et al.*, 1966). We would expect that the c.d. should also be identical. The consistent picture that emerges from our analysis supports this assumption. The same assumption was also made by Blum *et al.* (1972) in studying the c.d. of tRNA.

Borer *et al.* (1973) attempted to obtain values of C_i from the c.d. of a range of short bihelical models. Where comparison was possible the results obtained did not always agree with the values of C_i obtained from bihelical RNA and its high-molecular-weight models. One possible reason for this discrepancy given by Borer *et al.* (1973) is that results obtained from the oligomers were not sufficiently precise to allow individual values of C_i to be calculated exactly. Thus the work of Borer *et al.* (1973) does not support assumption (4) but does not necessarily challenge its validity.

(5) From the above assumptions, the c.d. of a bihelical RNA species having a mole fraction f_G of guanine residues is given by eqn. (4):

$$\Delta\varepsilon_{f_G}(\lambda) = af_G^2 + bf_G + c \qquad (4)$$

where a, b and c are constants (see the Appendix).

The c.d. of the bihelical parts of rRNA is given by eqn. (5):

$$\Delta\varepsilon_{bh}(\lambda) = f_{bh}\,\Delta\varepsilon_{f_G}(\lambda) \qquad (5)$$

where f_{bh} is the fraction of residues that are base-paired and $\Delta\varepsilon_{f_G}$ is the c.d. of the bihelical analogue having the appropriate value of f_G.

Table 1. *Comparison of the nearest-neighbour frequencies calculated from our empirical estimation of the nucleotide composition of the bihelical parts of E. coli S-rRNA with the nearest-neighbour frequencies found in the model of secondary structure based on the known primary sequence (Ehresmann et al., 1972)*

Sets of nearest neighbours	→ → / AA UU / : : / UU AA / ← ←	→ → / AU UA / : : / UA AU / ← ←	→ → / GG CC / : : / CC GG / ← ←	→ → / GC CG / : : / CG GC / ← ←	→ → → → / AG GA UC CU / : : : : / UC CU AG GA / ← ← ← ←	→ → → → / AC CA UG GU / : : : : / UG GU AC CA / ← ← ← ←
Appropriate model polynucleotides	Poly(A)·poly(U)	Poly(U-A)·poly(A-U)	Poly(G)·poly(C)	Poly(G-C)·poly(C-G)	Poly(A-G)·poly(U-C)	Poly(A-C)·poly(U-G)
Nearest-neighbour frequency found in model based on primary structure	0.090	0.082	0.205	0.128	0.268	0.224
Nearest-neighbour frequency calculated for 55% G+C base-pairs	0.101	0.101	0.151	0.151	0.248	0.248

(6) Eqn. (5) does not take into account the c.d. of G·U base-pairs. Where necessary the c.d. of G·U base-pairs is regarded as the mean of the appropriate G·C and A·U contribution.

(7) End effects are neglected in the derivation of eqn. (5), i.e. no special allowance was made for base-pairs located at the ends of a bihelical region.

(8) The nucleotide composition of the bihelical parts of rRNA was computed from the dispersion of the hypochromic effect (Cox, 1970*a*) according to eqn. (6):

$$\delta f_{A\cdot U}/\delta f_{G\cdot C} = 0.75(\delta\varepsilon_{260}/\delta\varepsilon_{280}) - 0.36 \qquad (6)$$

where $\delta f_{A\cdot U}$ and $\delta f_{G\cdot C}$ are respectively the mole fractions of A·U and G·C base-pairs, and $\delta\varepsilon_{260}$ and $\delta\varepsilon_{280}$ are the increments in ε at 260 and 280nm respectively that are found on 'melting out' secondary structure in a solvent that allows the transition from the native partly bihelical form to an amorphous form to be observed.

Estimation of the c.d. of single-stranded parts

(9) In principle the c.d. of the single-stranded parts may be computed from a library of spectra of dinucleoside monophosphates. However, Blum *et al.* (1972) concluded that these compounds are not good models for the corresponding interactions in longer molecules, and they used an empirical method to obtain $\Delta\varepsilon_{ss}$. We also sought an empirical method for estimating $\Delta\varepsilon_{ss}$. The c.d. spectrum ($\Delta\varepsilon_{denat.}$) of RNA measured in solvents that diminished bihelical secondary structure was considered to be the sum of two contributions, namely $\Delta\varepsilon_{ss}$ arising from residues located in single-stranded regions in the native state and $\Delta\varepsilon_{ex\text{-}bh}$ arising from residues located in bihelical parts in the native state (see eqn. 7):

$$\Delta\varepsilon_{denat.} = \Delta\varepsilon_{ss} + \Delta\varepsilon_{ex\text{-}bh} \qquad (7)$$

(10) The contribution of tertiary structure to c.d. was regarded as an enhancement of $\Delta\varepsilon_{ss}$, i.e.

$$T \propto \Delta\varepsilon_{ss} = t\Delta\varepsilon_{ss}$$

(11) Provided that the overall nucleotide composition of the single-stranded parts does not differ greatly from that of the whole molecule, then:

$$\Delta\varepsilon_{ss} \simeq (1 - f_{bh})\,\Delta\varepsilon_{denat.} \qquad (8)$$

The overall nucleotide composition of several rRNA species and the nucleotide composition of the single-stranded parts calculated from estimates of f_{bh} are compared in Table 3, and support this assumption. Hence:

$$\Delta\varepsilon_{ss} + T = (1 - f_{bh})\,\Delta\varepsilon_{denat.} + t\Delta\varepsilon_{denat.}$$
$$= Y\Delta\varepsilon_{denat.} \qquad (9)$$

(12) Two methods were used for preparing single-stranded non-base-paired (denatured) rRNA. First,

dialysis against 0.1 mM-EDTA was used to 'melt out' bihelical structure. Secondly, to ensure that complete denaturation was achieved, the dialysed solution was made 1% in formaldehyde, heated to 95°C and cooled, and electrolyte was added. Reaction of RNA with formaldehyde was shown to cause a small red shift in the c.d. compared with the c.d. obtained after the dialysis step (cf. Stevens, 1974).

(13) The two reference spectra $\Delta\varepsilon_{f_G}(\lambda)$ and $\Delta\varepsilon_{\text{denat.}}(\lambda)$ are related to the observed c.d. $\Delta\varepsilon$ by eqn. (10):

$$\Delta\varepsilon(\lambda) = f_{bh}\Delta\varepsilon_{f_G}(\lambda) + Y\Delta\varepsilon_{\text{denat.}}(\lambda) \qquad (10)$$

The unknown quantities f_{bh} and Y were computed both by regression analysis by using the Hewlett–Packard STAR subroutine and by a numerical procedure whereby the c.d. was calculated ($\Delta\varepsilon_{\text{calc.}}$) for a wide range of values of f_{bh} and Y and the values yielding the best fit were deduced. The fit between observed and calculated curves was defined according to eqn. (11):

$$\text{Fit} = \sqrt{\sum_1^N (\Delta\varepsilon_{\text{calc.}} - \Delta\varepsilon)^2 \Big/ \sum_1^N \Delta\varepsilon^2} \qquad (11)$$

The 'fit' defined by eqn. (11) is the average fractional deviation between measured and calculated values estimated at N wavelengths ($N \simeq 20$ in these experiments). Values of fit of 0.1 are found for different samples of the same species.

Assessment of the errors in the estimate of f_{bh}

We estimate that the overall limits in our estimates of f_{bh} are ±20%. Assumption (7) on end effects is the most difficult to assess for errors. The length of bihelical regions appears to be 12–15 base-pairs on average, i.e. one-sixth of base-pairs are terminal. If these terminal base-pairs make no contribution to $\Delta\varepsilon_{bh}$ then f_{bh} will be underestimated by one-sixth, whereas if the contribution of terminal base-pairs is twice that of internal base-pairs, f_{bh} will be overestimated by one-sixth. On this basis the limits would be ±0.1 when $f_{bh} = 0.6$. The calculation of $\Delta\varepsilon_{bh}$ is relatively insensitive to errors in f_G within the range f_G 0.15–0.35 because the major contributions to the spectrum arise from neighbouring A·U and G·C base-pairs (see Table 1). An error of 5% in f_G gives rise to an error of, at most, 5% in f_{bh}.

Values of f_{bh} do not depend on the absolute values of $\Delta\varepsilon_{\text{denat.}}$, but on the form of the spectrum; a shift of ±3 nm in the spectrum gives rise to differences of ±0.05 in f_{bh}. The curve-fitting procedure appears to be valid, since the contours obtained when the 'fit' was calculated for different values of f_{bh} and Y (see below) reveal a clearly defined best fit. The limit overall in the absolute values of f_{bh} arising from the various assumptions appears to be ±20% (e.g. $f_{bh} = 0.6 \pm 0.12$). When f_{bh} was calculated from the observed c.d. spectra (seven or more replicates) the standard deviation was found to be ±0.05.

The greatest uncertainty in the estimates of f_{bh} arises from the limitations of the theory. Combining the errors from experiment and theory we estimate that the absolute value of f_{bh} is accurate to ±15%. Relative values of f_{bh} are probably more precise because the limitations of the theoretical analysis are likely to introduce a systematic error, e.g. errors arising through neglecting end effects may consistently lead to either an underestimate or an overestimate of f_{bh}. We conclude that the relative values of f_{bh} obtained for the rRNA species studied are more accurate (±8%) than the estimated absolute values (±15%).

Calculation of the hypochromism of rRNA species

To provide an independent check on the estimates of f_{bh} and Y obtained from c.d. measurements, an equation analogous to eqn. (10) was used to calculate the hypochromism of rRNA, namely:

$$(\varepsilon_{am} - \varepsilon) = f_{bh}(\varepsilon_{am} - \varepsilon_{bh}) + Y(\varepsilon_{\text{HCHO(95°C)}} - \varepsilon_{\text{HCHO}}) \qquad (12)$$

where ε is the value for native RNA, ε_{am} is extinction at elevated temperatures of 'amorphous' rRNA, ε_{bh} is the extinction of the appropriate bihelical analogue, $\varepsilon_{\text{HCHO}}$ is the extinction found at approx. 25°C after heating at 95°C in the presence of 1% formaldehyde; and $\varepsilon_{\text{HCHO(95°C)}}$ is the extinction found at 95°C in 1% formaldehyde. $\varepsilon_{am} - \varepsilon_{bh}$ was calculated on the basis of the assumption that the values of $\varepsilon_{am} - \varepsilon_{bh}$ at 260 nm are 4500 $l \cdot mol^{-1} \cdot cm^{-1}$ for an A·U base-pair and 1500 $l \cdot mol^{-1} \cdot cm^{-1}$ for a G·C base-pair. The corresponding values at 280 nm were −200 $l \cdot mol^{-1} \cdot cm^{-1}$ for an A·U base-pair and 3400 $l \cdot mol^{-1} \cdot cm.^{1}$ for a G·C base-pair. The contributions to hypochromism of base-paired residues and residues 'stacked' in single-stranded regions are very similar, so that measurements of hypochromism alone are not sufficient to lead to unambiguous values of f_{bh}. The ratio of observed hypochromism to hypochromism of bihelical analogue measures both f_{bh} and f_{ss} (the fraction of residues 'stacked' in single-stranded regions). Provided that a residue that is 'stacked' in a single-stranded part makes the same contribution to $\Delta\varepsilon$ as if it were stacked in a base-paired region, then:

$$f_{bh} + f_{ss} = (\varepsilon_{am} - \varepsilon)/(\varepsilon_{am} - \varepsilon_{bh}) \qquad (13)$$

An estimate of f_{bh} obtained by c.d. measurements allows f_{ss} to be calculated.

Methods

The isolation of the subribosomal particles has been described previously (Cox *et al.*, 1973*b*). The rRNA was precipitated as the guanidinium salt by

ethanol (Cox, 1968) and dissolved in 10mM-NH_4Cl/0.1mM-$MgCl_2$/10mM-sodium phosphate buffer, pH7. Rabbit reticulocyte L-rRNA was hydrolysed with ribonuclease T_1 (EC 3.1.4.8); the G+C-rich fragments were isolated by zonal centrifugation (Cox *et al.*, 1973*a*) and then dissolved in the same buffer as above.

The rRNA was unfolded by dialysis overnight against 0.1mM-EDTA (sodium salt), pH7, and for a further 4h against two changes of deionized water adjusted to pH7.0 with NaOH. Denaturation of the rRNA was completed by heating 3ml of unfolded rRNA at 97°C for 3min in the presence of 1% deionized formaldehyde. After cooling in ice the standard buffer conditions were obtained by adding 30μl of 1M-NH_4Cl/1M-sodium phosphate buffer, pH7, and 3μl of 0.1mM-$MgCl_2$ to the formaldehyde-treated rRNA solution. After dialysis, a sample of rRNA was renatured by addition of 50μl of 1M-NH_4Cl/1M-sodium phosphate buffer, pH7, and 5μl of 0.1M-$MgCl_2$ to 5ml of the rRNA in water.

The u.v. absorption of all solutions was measured in a Pye–Unicam SP.500 spectrophotometer. The c.d. of a solution of native rRNA and subribosomal particles that had E_{260}^{1mm} not more than 1.3 $l \cdot mol^{-1} \cdot mm^{-1}$ was measured in a 1mm-path-length quartz cell in a Rousset–Jouan Dichrograph (model CD185). To increase accuracy, the c.d. of the same solution was also measured above 285nm in a 1cm-path-length cell; this gives a 10-fold increase in sensitivity. For the single-stranded forms of rRNA, the c.d. of solutions with E_{260}^{1cm} not more than 1.3 $l \cdot mol^{-1} \cdot cm^{-1}$ was measured in 1cm-path-length cells only.

All c.d. measurements were converted into extinction per g-atom of P by assuming a molar extinction of 7750 $l \cdot g\text{-}atom^{-1} \cdot cm^{-1}$ for native rRNA.

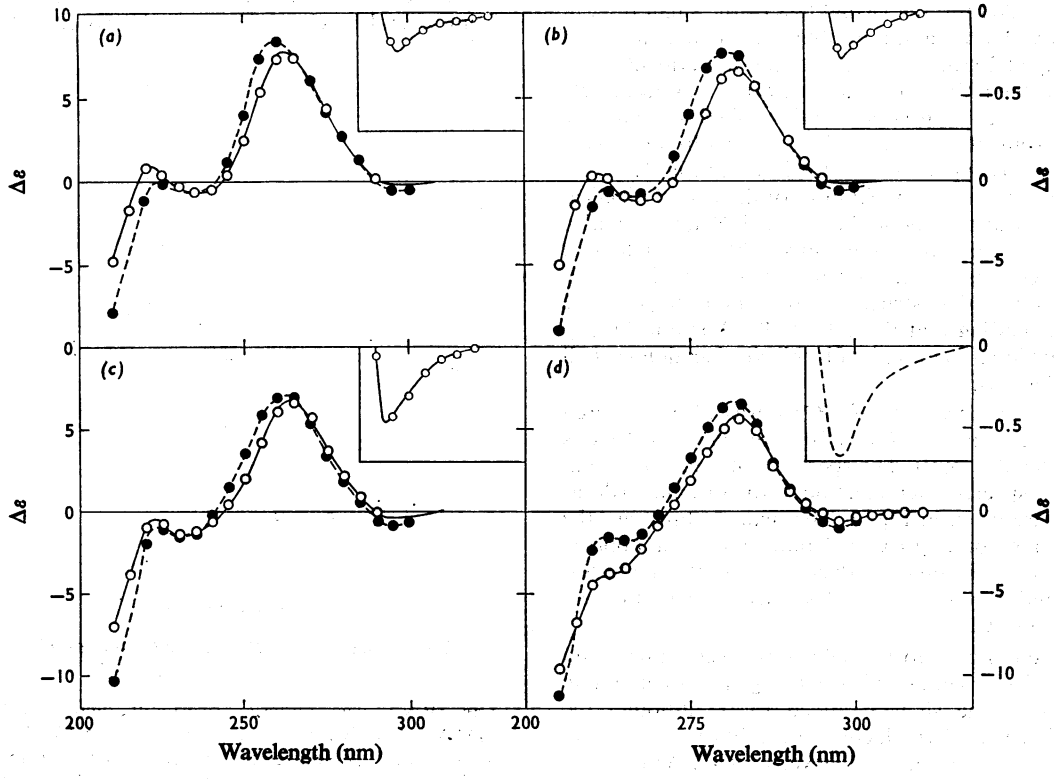

Fig. 1. *C.d. spectra of four rRNA species with base compositions ranging from 42% to 78% G+C (Cox et al., 1973a) compared with the c.d. spectra expected for bihelical RNA of the same base composition as the bihelical regions of the respective rRNA species (see the Appendix)*

The c.d. was measured in 10mM-NH_4Cl/0.1mM-$MgCl_2$/10mM-sodium phosphate buffer, pH7, in 1mm-path-length cells ($E_{260} = 1.2\ l \cdot mol^{-1} \cdot mm^{-1}$); accuracy was increased by using 1cm-path-length cells ($E_{260} = 12\ l \cdot mol^{-1} \cdot cm^{-1}$) in that region of the spectrum above 285nm where the absorbance was low. (*a*) *D. melanogaster* L-rRNA (42% G+C); (*b*) *E. coli* L-rRNA (55% G+C); (*c*) rabbit reticulocyte L-rRNA (67% G+C); (*d*) G+C-rich fragment of rabbit L-rRNA (78% G+C). ●, C.d. spectrum calculated for authentic bihelical RNA; ○, c.d. spectra of native rRNA.

Results

The c.d. spectra, in the near u.v., of several rRNA species with base compositions ranging from 42% to 78% G+C are given in Fig. 1, together with the spectra calculated for bihelical RNA having the same nucleotide composition as the bihelical parts of the respective rRNA species. The solvent used was 10mM-NH_4Cl/0.1mM-$MgCl_2$/10mM-sodium phosphate buffer, pH7; this was chosen because it is suitable for active subparticles and it has a comparatively low extinction at 220nm. The spectra of bihelical RNA depends on base composition and a similar dependence on % G+C was found for the c.d. spectra of the rRNA species, providing further evidence that the partly bihelical nature of rRNA is reflected in the c.d. spectrum (cf. Yang & Samejima, 1969; Gratzer & Richards, 1971). The obvious changes that occur in the c.d. spectra of the bihelical RNA species as the base composition changes from 42% to 78% G+C are a diminution of the peak at approx. 260nm, the virtual loss of the small peak at approx. 220nm and a doubling in the magnitude of the dip at 295nm. The same trends are evident in the c.d. of the rRNA. The c.d. at 295nm was accurately measured at high concentration of rRNA, and the enhancement of the minimum with increasing % G+C is apparent from the insets in Fig. 1.

Although the main features of the c.d. of bihelical RNA are also found in the c.d. of rRNA, there is also a contribution over the range 230–265nm to c.d. from residues in single-stranded regions and possibly also from tertiary structure. This is indicated in Fig. 1 by the finding that the c.d. of rRNA is not directly proportional to the c.d. of its bihelical analogue at all wavelengths.

The c.d. spectrum of rRNA was also measured after denaturation (i.e. after the bihelical regions were 'melted out'). The spectra obtained for several rRNA species after reaction with formaldehyde at 97°C are given in Fig. 2. The main features are the maximum of approx. 5 $l \cdot mol^{-1} \cdot cm^{-1}$ at approx. 270nm that is almost independent of base composition and the increase in half-bandwidth with increasing % G+C.

Reaction with formaldehyde is a very simple and convenient method of producing and maintaining rRNA in the single-stranded form, although the reaction with formaldehyde does have an effect on the c.d. spectra (see, e.g., Stevens, 1974). With rRNA the magnitude of the maximum is scarcely affected, but the band undergoes a red shift of about 3nm relative to the spectra of rRNA unfolded in low ionic strength buffer (see Fig. 3). The shift in the c.d. spectrum has to be borne in mind in attempts to relate the spectra of the denatured rRNA and bihelical RNA to that of native rRNA. The advantage of using formaldehyde as a denaturant is that complete denaturation can be ensured and the c.d. can be measured in the same ionic conditions as were used for native rRNA.

The c.d. spectrum of rRNA unfolded in a low-ionic-strength solvent was also measured for the four rRNA species studied in detail. The advantage of this procedure is that chemical modification of the base residues is avoided, but the disadvantages are that the denaturation may not be complete and that a small change in pH, e.g. to below 6, is sufficient to lead to protonization of adenine and cytosine residues (Cox & Littauer, 1963) and thereby affect the c.d. spectrum. These effects were minimized by dialysis against 0.1mM-EDTA, pH7. This procedure not only leads to the chelation of bivalent cations, which even in low amounts stabilize bihelical structures, but also buffers the solution near to neutral pH. *E. coli* rRNA is denatured in solutions free of bivalent cations where the concentration of Na^+ ions is 0.5mM or less (Cox & Littauer, 1962).

The c.d. of at least seven samples of rRNA isolated from several batches of a particular species of cells

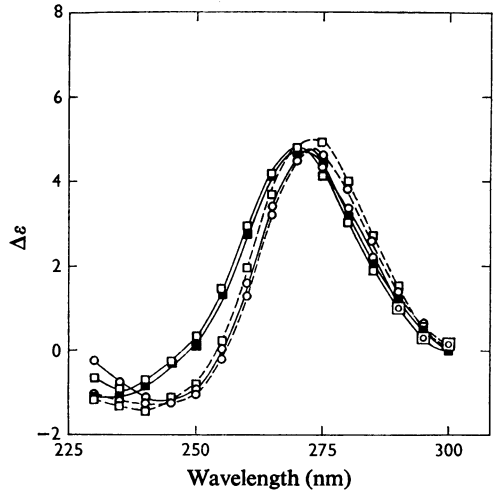

Fig. 2. *C.d. spectrum of rRNA after heating at 95°C in the presence of 1% formaldehyde*

The rRNA was dialysed overnight against 0.1mM-EDTA, pH7, before heating for 3min to 97°C in the presence of 1% deionized formaldehyde. The solution was rapidly cooled in ice, adjusted to 10mM-NH_4Cl/0.1mM-$MgCl_2$/10mM-sodium phosphate buffer, pH7, and the c.d. spectrum measured. ○--○, *E. coli* S-rRNA (53.7% G+C); ○——○, *E. coli* L-rRNA (55% G+C); □--□, rabbit reticulocyte S-rRNA (59.5% G+C); □——□, rabbit reticulocyte L-rRNA (67% G+C); ■——■, G+C-rich fragment of rabbit L-rRNA (78% G+C). The values in parentheses refer to the overall base composition of the rRNA (Cox *et al.*, 1973*a*,*b*).

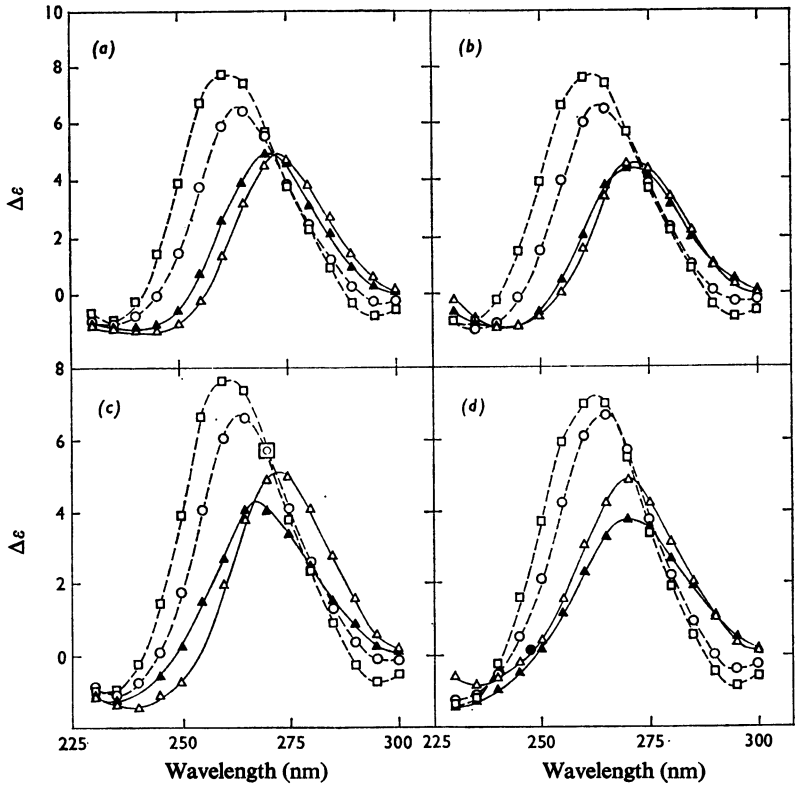

Fig. 3. *C.d. spectra of rRNA of E. coli and rabbit reticulocyte in the single-stranded state induced by preheating the rRNA with formaldehyde*

The rRNA was dialysed overnight against 0.1mM-EDTA, pH7, to remove Mg^{2+} ions, heated at 97°C for 3min in 1% deionized formaldehyde, cooled in ice and the solvent adjusted to 10mM-NH_4Cl/0.1mM-$MgCl_2$/10mM-sodium phosphate buffer, pH7. For comparison, the c.d. spectra calculated for bihelical RNA of 55% G+C (*E. coli*) and 67% G+C (rabbit reticulocyte), by the method described in the Appendix (Cox & Hirst, 1976), are included together with the c.d. spectrum of the native rRNA. (*a*) *E. coli* S-rRNA; (*b*) *E. coli* L-rRNA; (*c*) rabbit reticulocyte S-rRNA; (*d*) rabbit reticulocyte L-rRNA. ○--○, Mean of seven observed c.d. curves of native rRNA; △——△, c.d. curve measured for rRNA after dialysis against EDTA; ▲——▲, c.d. curve of rRNA measured after reaction with deionized formaldehyde; □--□, c.d. curve calculated for bihelical RNA of the same base composition as the bihelical regions of the respective rRNA.

was measured, and the dispersion of the standard deviations of the observed values is indicated in Figs. 4 and 5. The range of fit (defined by eqn. 11) for different samples compared with the mean was 0.02–0.08. The procedure of fitting the observed curve with a combination of contributions from bihelical and single-stranded regions (eqn. 10) led to a best fit of approx. 0.1 (see Table 2), a value comparable with extreme values found for different preparations of the same rRNA species. The variation of fit with f_{bh} and Y is given in Fig. 6, together with the values of f_{bh} and Y calculated by regression analysis. The differences between the observed and calculated values of $\Delta\varepsilon(\lambda)$ lie generally within 2 standard deviations; however, the difference between the observed and calculated values of $\Delta\varepsilon(\lambda)$ is systematic rather than random.

It is evident from Table 2 that eqn. (10) may be used to fit the observed c.d. of the range of rRNA species studied. The values of fit range from 0.05 to 0.12; this is the fit expected between different samples of the same species of RNA and is in general better than the fit between the observed and calculated c.d. of tRNA (Blum *et al.*, 1972). The red shift in c.d. of rRNA on reaction with formaldehyde could lead to an overestimate of f_{bh} of no more than 0.05, whereas an underestimate would be obtained if $\Delta\varepsilon_{aq.}$ includes a contribution from base-paired residues. The values

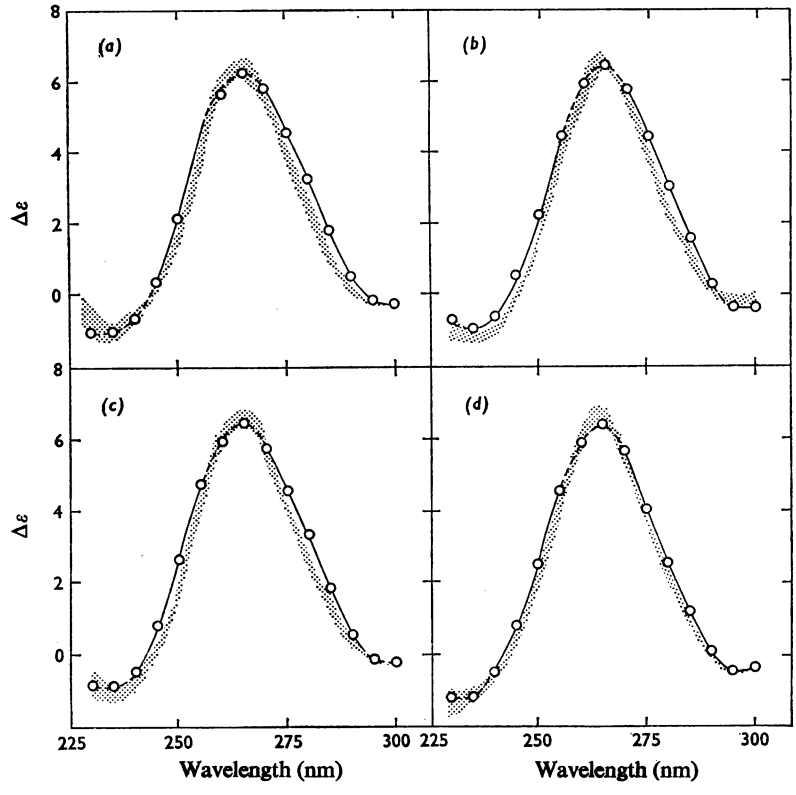

Fig. 4. *Comparison of the observed and calculated c.d. spectra for the rRNA of rabbit reticulocyte and E. coli*

Eqn. (10) was solved for f_{bh} and Y by a least-squares analysis by using the assumption that the c.d. spectrum of formaldehyde-treated rRNA is the same as that of the single-stranded regions. The spectrum calculated by using these values of f_{bh} and Y was divided into two types of regions, namely those values that lie within 1 standard deviation of the mean observed value (O--O) and those values that lie outside this limit (O——O). The stippled area indicates the dispersion of 1 standard deviation from the mean observed spectrum. (*a*) *E. coli* S-rRNA; (*b*) *E. coli* L-rRNA; (*c*) rabbit reticulocyte S-rRNA; (*d*) rabbit reticulocyte L-rRNA.

of f_{bh} calculated by using $\Delta\varepsilon_{denat.} = \Delta\varepsilon_{aq.}$ and $\Delta\varepsilon_{denat.} = \Delta\varepsilon_{HCHO}$ are likely to represent respectively the minimum and maximum values.

The nucleotide composition of the single-stranded regions may be computed if f_{bh} and the nucleotide composition of the bihelical parts are known (see Table 3). The approximation that $\Delta\varepsilon_{denat.} \propto \Delta\varepsilon_{ss}$ is likely to be most satisfactory for rabbit rRNA since the nucleotide composition of the single-stranded parts is reflected in the overall nucleotide composition. This could account for the better 'fit' between calculated and observed values of c.d. The single-stranded regions of S-rRNA and L-rRNA of *E. coli* appear to be guanine-rich compared with the composition overall.

The values of f_{bh} derived from the c.d. measurements agree with other measurements. This is shown by the agreement between the observed values of hypochromism and those calculated by means of eqn. (12) (see Table 4). The c.d. of S-rRNA of *E. coli* is an important reference compound for c.d. studies because its primary structure is largely known (Ehresmann *et al.*, 1972). Few physical measurements yielding quantitative information about the number of base-pairs (f_{bh}) etc. of *E. coli* S-rRNA have been made; instead, results obtained from studies of an unfractionated mixture of S-rRNA and L-rRNA (1:2, w/w) have been extrapolated to S-rRNA, even though it is clearly the minor component. We have found no conflict between the values of f_{bh} obtained for S-rRNA and L-rRNA (Table 2) and those reported for the unfractionated mixture of S-rRNA and L-rRNA. The data for *E. coli* S-rRNA (see Table 5) are consistent with the model of secondary structure proposed on the basis of primary structure (Ehresmann *et al.*, 1972).

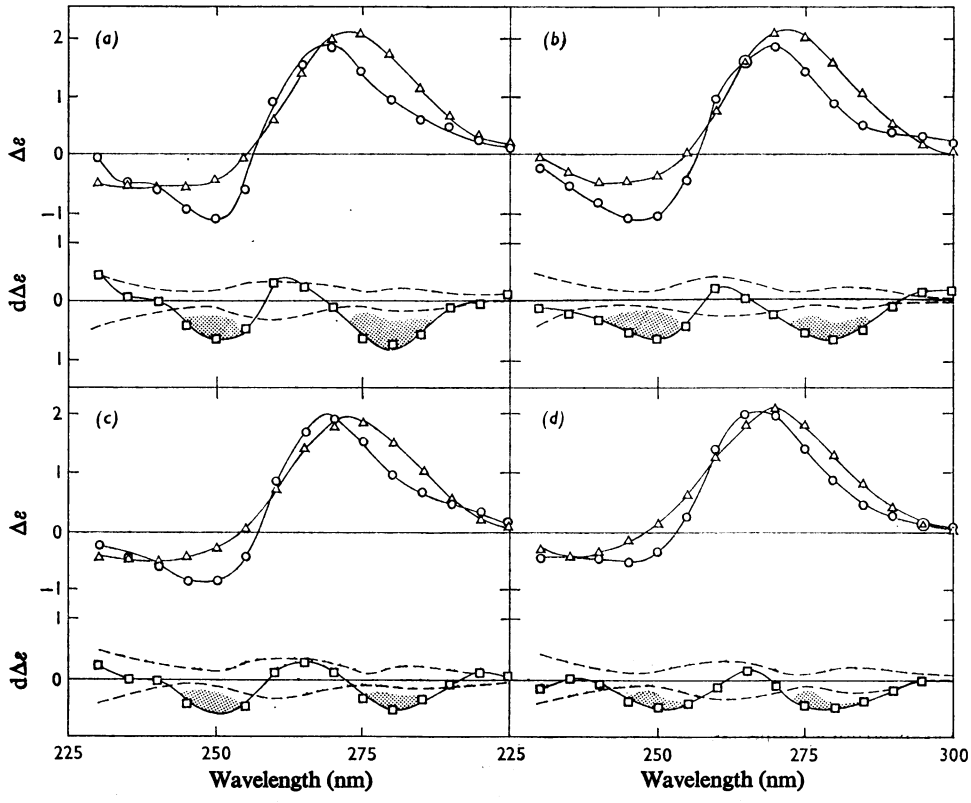

Fig. 5. *Estimated c.d. spectra of the single-stranded regions obtained by two methods and the difference between the observed and calculated c.d. spectra of rRNA*

(*a*) *E. coli* S-rRNA; (*b*) *E. coli* L-rRNA; (*c*) rabbit reticulocyte S-rRNA; (*d*) rabbit reticulocyte L-rRNA. □, Difference (d$\Delta\varepsilon$) between the calculated and observed spectra. The broken line (-----) is the dispersion of 1 standard deviation (from three series of seven replicate measurements); the stippled areas indicate values of d$\Delta\varepsilon$ greater than 2 standard deviations. ○, Contribution from single-stranded regions assumed to be the difference between the observed c.d. and the bihelical contribution, i.e. $\Delta\varepsilon - f_{bh}\Delta\varepsilon_{rG}$. △, Contribution from single-stranded regions assumed to be a proportion of the c.d. spectrum of rRNA denatured with formaldehyde, i.e. $Y\Delta\varepsilon_{HCHO}$.

Comparison of the c.d. spectrum of the rRNA moiety of the subribosomal particle with that of rRNA either dissociated from the proteins by means of 1% sodium dodecyl sulphate or isolated as the guanidinium salt show that all three spectra are very similar, except possibly in the region of 295nm (see Fig. 7). The contribution to c.d. of bihelical and single-stranded structures of rRNA in the subribosomal particle and in free solution differed by no more than 5%, judged by the values of f_{bh} and Y. Thus combination of rRNA with protein appears to have no more than a small effect overall on the conformation of rRNA as judged by c.d. measurements.

Discussion

It was noted in the introduction that L-rRNA from different species varies widely in nucleotide composition (see, e.g., Lava-Sanchez *et al.*, 1972), and so the question arises of what kinds of secondary structure are generated by these different primary sequences. It was also noted that the spectra of *D. melanogaster* L-rRNA (42% G+C) and fragments of rabbit L-rRNA (approx. 78% G+C) were sufficiently different to need explanation. Before this present study was undertaken the c.d. of rRNA had been analysed on the basis of the assumption (Gratzer & Richards, 1971) that the c.d. of the bihelical parts of rRNA, irrespective of their nucleotide composition,

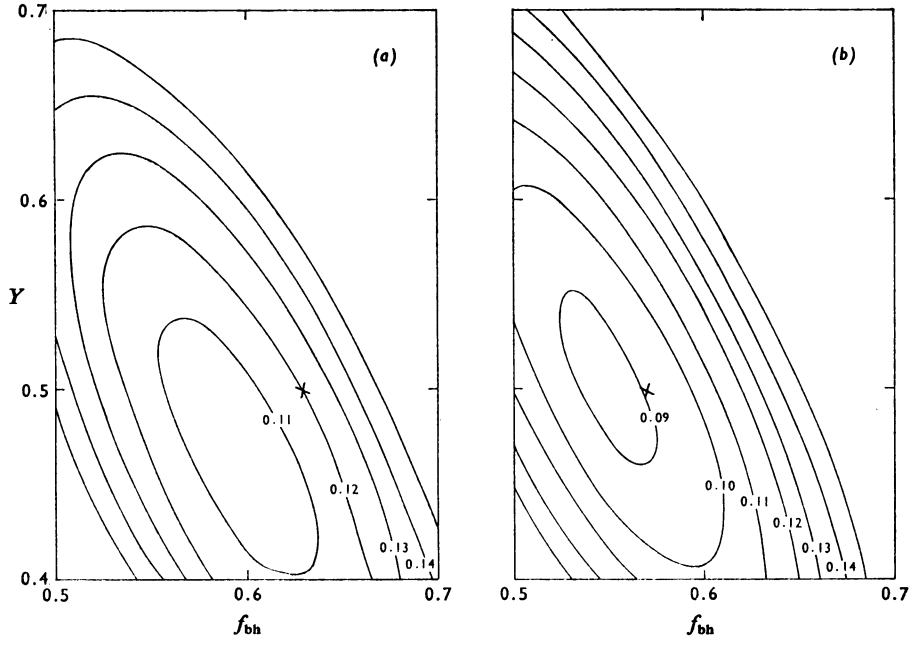

Fig. 6. *Variation in the fit of the observed and calculated spectra of (a) E. coli L-rRNA and (b) E. coli S-rRNA as the parameters f_{bh} and Y in eqn.* (10) *are varied*

The calculated spectrum is defined as:

$$\Delta\varepsilon_{calc.} = f_{bh}\Delta\varepsilon_{fG} + Y\Delta\varepsilon_{aq.} \quad (10a)$$

where $\Delta\varepsilon_{fG}$ is the theoretical contribution of the bihelical analogue at a given wavelength and $\Delta\varepsilon_{aq.}$ is the c.d. observed at the same wavelength for the rRNA species after dialysis against EDTA (see the text for further explanation). The crosses mark the values of f_{bh} and Y obtained by using the least-squares programme from the STAR subroutine of a Hewlett–Packard 3000 computer. The optimum values obtained by the least-squares method for both f_{bh} and Y differ by about 2% from the values deduced on the basis of the best fit. The contours denote points of equal fit the value of which is shown by the numbers given in the Figure.

Table 2. *Estimates of the extent of bihelical secondary structure of rRNA obtained by analysis of c.d. spectra*

Data for % G+C of bihelical regions were taken from Cox *et al.* (1973*b*), except those for the G+C-rich fragment (see Cox *et al.*, 1973*a*). The parameters f_{bh} and Y were chosen by solving the equation:

$$\Delta\varepsilon_{obs.} = f_{bh}\Delta\varepsilon_{fG} + Y\Delta\varepsilon_{ss}$$

by using the least-squares linear analysis of the Hewlett–Packard STAR subroutine. $\Delta\varepsilon_{ss}$ was estimated from the c.d. of the rRNA either after heating with formaldehyde ($\Delta\varepsilon_{HCHO}$) or in low-ionic-strength solvent ($\Delta\varepsilon_{aq.}$). The fit was calculated by means of eqn. (11).

Species	% G+C of the bihelical regions	Parameters calculated by using $\Delta\varepsilon_{HCHO}$ as reference for single strands			Parameters calculated by $\Delta\varepsilon_{aq.}$ as reference for single strands		
		f_{bh}	Y	Fit	f_{bh}	Y	Fit
E. coli S-rRNA	53.5	0.65	0.44	0.117	0.57	0.50	0.091
E. coli L-rRNA	55	0.66	0.43	0.103	0.63	0.50	0.120
Rabbit reticulocyte S-rRNA	55	0.66	0.38	0.084	0.50	0.68	0.070
Rabbit reticulocyte L-rRNA	67	0.66	0.44	0.084	0.55	0.72	0.084
G+C-rich fragment of rabbit L-rRNA	78	0.72	0.26	0.074	0.61	0.40	0.047

Table 3. ***Estimated nucleotide composition of the single-stranded parts of rRNA***

Species	Base composition by chemical analysis* (%) A	U	G	C	% G+C in bihelical regions†	Calculated base composition of single-stranded regions‡ (%) A	U	G	C
E. coli S-rRNA	24.8	21.5	31.0	22.7	54.5	27.8±0.8	17.9±0.7	39.6±0.6	14.7±1.9
E. coli L-rRNA	25.4	19.6	33.5	21.5	55	31.2±1.7	13.7±1.3	45.6±2.3	9.5±2.6
Rabbit reticulocyte S-rRNA	20.5	20.0	30.7	28.8	55	16.5±0.8	15.1±1.0	37.1±1.4	31.3±0.5
Rabbit reticulocyte L-rRNA	16.4	16.6	35.3	31.6	68.5	17.7±0.3	18.3±0.4	37.6±0.5	26.4±1.4
G+C-rich fragment of rabbit L-rRNA	13.3	10.7	38.3	37.7	78	19.4±1.5	9.7±0.2	36.4±0.4	34.5±1.0

* Data for the rRNA species are taken from Cox (1970*b*) and those for the G+C-rich fragment of rabbit L-rRNA from Cox *et al.* (1973*a*).

† Data for rRNA species are taken from Cox *et al.* (1973*b*) and those for the G+C-rich fragment of rabbit L-rRNA from Cox *et al.* (1973*a*).

‡ Assuming 66±5% bihelix for the rRNA species and 72±5% bihelix for the G+C-rich fragment of rabbit L-rRNA (see Table 2).

Table 4. *Comparison of the observed hypochromism of rRNA with calculated values based on estimates of f_{bh} and Y obtained from c.d. measurements (see Table 2)*

Species	% G+C from chemical analysis*	% G+C in bihelical regions*	Wavelength (nm)	Hypochromic effect at 260 and 280nm† $(\varepsilon_{am}-\varepsilon_{bh})\pm 100$ (l·mol^{-1}·cm^{-1}) Calculated values: Based on $\Delta\varepsilon_{HCHO}$‡	Calculated values: Based on $\Delta\varepsilon_{aq}$.§	Observed values	$\frac{\varepsilon_{am}-\varepsilon}{\varepsilon_{am}-\varepsilon_{bh}}\simeq(f_{bh}+f_{ss})$‖
E. coli S-rRNA	54	53.5±1	260	2284	2170	2300±100	0.86±0.03
			280	1464	1371	1500±100	0.80±0.03
E. coli L-rRNA	55	55 ±1	260	2274	2261	2450±100	0.81±0.03
			280	1497	1506	1500±100	0.80±0.03
Rabbit reticulocyte S-rRNA	59.5	55 ±1	260	2221	2108	2050±100	0.75±0.03
			280	1446	1345	1350±100	0.72±0.03
Rabbit reticulocyte L-rRNA	67	68.5±1	260	2193	2182	2150±100	0.83±0.03
			280	1924	1954	1800±100	0.78±0.03
G+C-rich fragment of rabbit L-rRNA	78	78 ±2	260	2084	1945	2000±100	0.93±0.03
			280	2119	1975	2300±100	0.87±0.03
D. melanogaster L-rRNA	42.1	39 ±2	260	2760¶	—	2750±100	0.83±0.03
			280	1060¶	—	1030±100	0.78±0.03

* The base composition of the rRNA was taken from Cox *et al.* (1973*b*) and that of the G+C-rich fragment of rabbit L-rRNA from Cox *et al.* (1973*a*).

† The equation $\varepsilon_{am}-\varepsilon=f_{bh}(\varepsilon_{am}-\varepsilon_{bh})+Y(\varepsilon_{am}-\varepsilon_{HCHO})$ was used, where ε is the observed value for native rRNA, ε_{am} is the value found at 95°C after all bihelical structure has 'melted', ε_{bh} is the extinction of the homologous bihelical RNA, and ε_{HCHO} is the extinction of the single-stranded form measured at 25°C after heating at 95°C in 1% formaldehyde.

‡ f_{bh} and Y were estimated by means of eqn. (10) by using the data for formaldehyde-treated rRNA.

§ f_{bh} and the single-stranded contribution Y in eqn. (10) were estimated by using the spectrum of rRNA obtained in a low-ionic-strength solvent.

‖ $\varepsilon_{am}-\varepsilon_{bh}$ was calculated on the basis of the assumption that $\varepsilon_{am}-\varepsilon_{bh}=4500$ l·mol^{-1}·cm^{-1} at 260nm for an A·U base-pair and that $\varepsilon_{am}-\varepsilon_{bh}=1500$ l·mol^{-1}·cm^{-1} at 260nm for a G·C base-pair. The values at 280nm were taken as −700 l·mol^{-1}·cm^{-1} for an A·U base-pair and 3400 l·mol^{-1}·cm^{-1} for a G·C base-pair.

¶ Based on values of $f_{bh}=0.65$ and $Y=0.45$.

is proportional to the average c.d. of several bihelical RNA species of approx. 40–50% G+C, i.e.:

$$\Delta\varepsilon_{bh}(\lambda)=f_{bh}\,\Delta\varepsilon^{\circ}(\lambda) \qquad (14)$$

where $\Delta\varepsilon^{\circ}(\lambda)$ is the average c.d. of the reference bihelical RNA species and is independent of f_G.

On the basis of this assumption, the differences in the c.d. of the L-rRNA species studied are attributable mainly to variations in f_{bh}, and it seems that 85% or more of the base residues of *D. melanogaster* L-rRNA form base-pairs, since the c.d. spectrum of this species is very similar to average c.d. spectrum

Table 5. *Comparison of the features of secondary structure of E. coli S-rRNA calculated from c.d. and other optical measurements with the features of the model based on primary sequence (Ehresmann et al., 1972)*

	f_{bh}	Fraction of G·C base-pairs of bihelical parts	Number of base-pairs per uninterrupted bihelical region	Number of residues per hairpin
Model based on primary sequence	0.63*	0.54†	3–10	28 (mean) 16–65 (range)‡
Empirical methods	0.61 ± 0.04	(mean) 0.55 ± 0.01 (range) 0.47–0.67	<17	25 ± 5§

* This value includes 0.06 for G·U base-pairs.
† Includes G·U base-pairs; a value of 0.60 is found if G·U base-pairs are discounted.
‡ The range includes three large loops (see Ehresmann *et al.*, 1972).
§ Calculated for rabbit S-rRNA, but we hold the view that the secondary structures of *E. coli* S-rRNA and rabbit reticulocyte S-rRNA have many features in common (Cox *et al.*, 1973*a*).

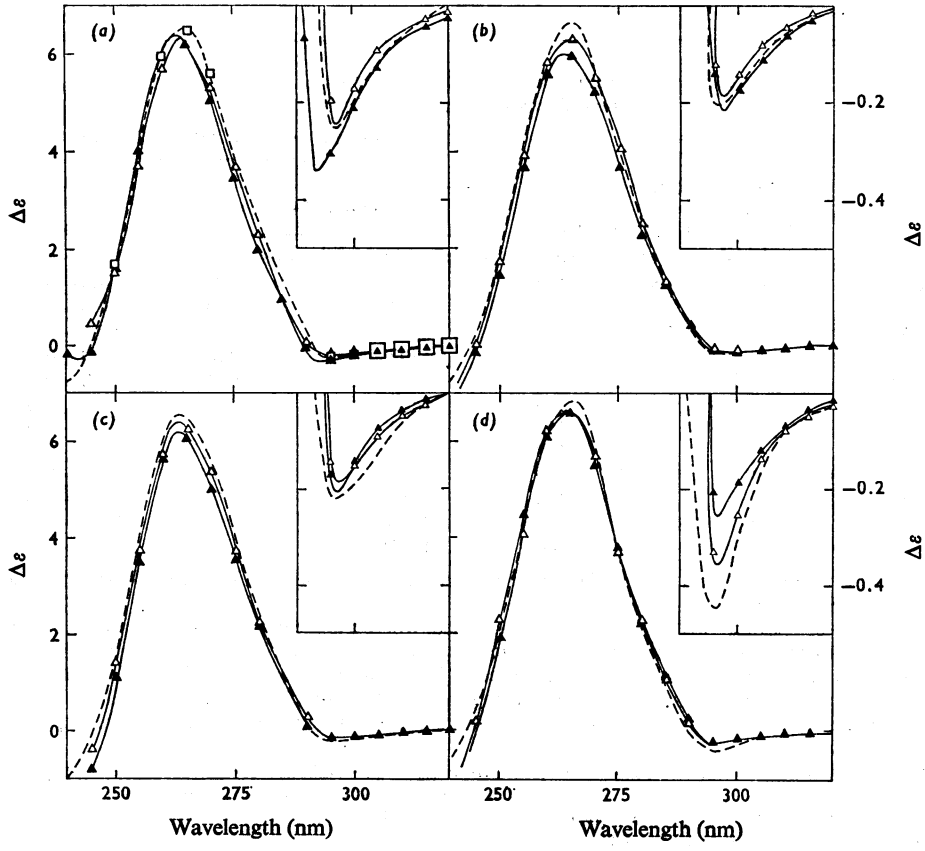

Fig. 7. *Comparison of the c.d. spectra of rRNA complexed in the sRS, rRNA dissociated from the subparticle by 1% sodium dodecyl sulphate and the free rRNA of the L-sRS and S-sRS of E. coli and rabbit reticulocytes*

The solvent in all experiments was 10mM-NH_4Cl/0.1mM-$MgCl_2$/10mM-sodium phosphate buffer, pH7. The spectrum was measured in 1mm-path-length cells ($E_{260} = 1.2\ l \cdot mol^{-1} \cdot mm^{-1}$), and, in addition, at wavelengths above 285nm the spectrum was also measured in 1cm-path-length cells ($E_{260} = 12\ l \cdot mol^{-1} \cdot cm^{-1}$) to increase the accuracy in measuring the dip at 295nm. (*a*) *E. coli* S-sRS; (*b*) rabbit reticulocyte S-sRS; (*c*) *E. coli* L-sRS; (*d*) rabbit reticulocyte L-sRS. ----, Free rRNA; ▲——▲, rRNA complexed in the intact subparticle; △——△, rRNA dissociated from ribosomal proteins by 1% sodium dodecyl sulphate.

deduced by Gratzer & Richards (1971) for bihelical RNA. In contrast, rabbit L-rRNA and its G+C-rich fragment appear to be much less ordered in their secondary structure, with fewer than 50% of residues forming base-pairs. It appears that L-rRNA species vary widely in their secondary structure, with the tendency for bihelical content to diminish as G+C content increases. This would be an important conclusion if it were confirmed. However, this conclusion conflicts with the view of secondary structure obtained by analysis of the hypochromic effect (e.g. Table 4).

Our own analysis, which takes into account the different contributions of A·U and G·C base-pairs to c.d., reveals a different picture, namely that the rRNA species studied, irrespective of their wide range in overall nucleotide composition (42–78% G+C), have much the same bihelical content. Thus the difference in the c.d. of *D. melanogaster* L-rRNA (42% G+C) and of fragments (78% G+C) of rabbit L-rRNA is largely attributable to the different contributions to c.d. of A·U and G·C base-pairs (see eqn. 4). This conclusion is in accord with the results of the analysis of the hypochromic effect (Table 4) and with the notion that L-rRNA species have features of secondary structure in common irrespective of the overall nucleotide composition (Cox *et al.*, 1973*a*; Godwin *et al.*, 1974).

There is no other evidence to support the analysis of *D. melanogaster* rRNA. However, there is accord between the results obtained from optical measurements (Table 5) with other studies in the case of *E. coli* S-rRNA, as mentioned above. The results of the c.d. analysis (Table 4) are also consistent with the known properties of the G+C-rich fragments of rabbit L-rRNA. Evidence for substantial base-pairing is inferred from the appearance of the fragments revealed by electron microscopy (Godwin *et al.*, 1974). The branched structures that are found for the G+C-rich fragments were first shown to be present in vertebrate L-rRNA and pre-rRNA by Wellauer & Dawid (1973). Further evidence that the G+C-rich L-rRNA fragments have a substantial degree of order is inferred from the resistance of these fragments (Cox *et al.*, 1973*a*) to hydrolysis by ribonuclease T_1 (EC 3.1.4.8). This enzyme catalyses the hydrolysis of the 3′-internucleotide linkage of guanine residues. On the basis of nucleotide composition the fragments would be expected to be very readily hydrolysed by this enzyme, and the high stability that is observed is attributed to the influence of secondary structure. The data inferred from optical properties (Table 5) are in accord with and extend our knowledge of these fragments gained from their morphology as seen in the electron microscopy and their resistance to ribonuclease T_1.

Finally, it appears that the conformation of rRNA within the subparticle has much the same bihelical content as rRNA in the same solvent, since f_{bh} and Y were the same within 5%, i.e. within the limits of experimental error. In two cases, namely *E. coli* S-sRS and rabbit reticulocyte L-sRS, a difference in $\Delta\varepsilon_{295}$ was found that was beyond experimental error. The observed change in $\Delta\varepsilon_{295}$ is comparable in magnitude with that found when Acridine Orange binds to yeast rRNA in 1.35M-KCl, pH7.6, at 22°C (Hoener *et al.*, 1973), conditions that favour intercalation of the dye between nucleotide residues. Interaction of Acridine Orange with rRNA has no measurable effect on $\Delta\varepsilon_{265}$ or hypochromicity, indicating that the dye induces little or no change in f_{bh}. It is clear from 'melting' studies (Cox *et al.*, 1973*b*) that the protein moiety does influence the thermal stability of the bihelical regions but does not significantly change the number of base-pairs. It appears that, except possibly at about 295nm, c.d. measurements have not yet proved to be a sensitive probe for RNA–protein interactions.

References

Arnott, S., Hutchinson, F., Spencer, M., Wilkins, M. H. F., Fuller, W. & Langridge, R. (1966) *Nature (London)* **211**, 227–232

Blum, A. D., Uhlenbeck, O. C. & Tinoco, I., Jr. (1972) *Biochemistry* **11**, 3248–3256

Borer, P. N., Uhlenbeck, O. C., Dengler, B. & Tinoco, I., Jr. (1973) *J. Mol. Biol.* **80**, 759–771

Cox, R. A. (1968) *Methods Enzymol.* **12B**, 120–129

Cox, R. A. (1970*a*) *Biochem. J.* **117**, 101–118

Cox, R. A. (1970*b*) *Biochem. J.* **120**, 539–548

Cox, R. A. & Hirst, W. (1976) *Biochem. J.* **155**, 292–295

Cox, R. A. & Littauer, U. Z. (1962) *Biochim. Biophys. Acta* **61**, 197–208

Cox, R. A. & Littauer, U. Z. (1963) *Biochim. Biophys. Acta* **72**, 188–202

Cox, R. A., Huvos, P. & Godwin, E. A. (1973*a*) *Isr. J. Chem.* **11**, 407–422

Cox, R. A., Pratt, H., Huvos, P., Higginson, B. & Hirst, W. (1973*b*) *Biochem. J.* **134**, 775–793

Ehresmann, C., Stiegler, P., Fellner, P. & Ebel, J.-P. (1972) *Biochimie* **54**, 901–967

Godwin, E., Cox, R. A. & Huvos, P. (1974) *Acta Biol. Med. Germ.* **33**, 733–752

Gratzer, W. B. & Richards, E. G. (1971) *Biopolymers* **10**, 2607–2614

Hoener, B. A., Sokoloski, T. D. & Mitscher, L. A. (1973) *Antimicrob. Ag. Chemother.* **4**, 455–458

Lava-Sanchez, P. A., Amaldi, F. & La Posta, A. (1972) *J. Mol. Evol.* **2**, 44–55

Schibler, U., Wyler, T. & Hagensbuschle, O. (1975) *J. Mol. Biol.* **94**, 503–517

Stevens, C. L. (1974) *Biopolymers* **13**, 1517–1533

Wellauer, P. & Dawid, I. (1973) *Proc. Natl. Acad. Sci. U.S.A.* **70**, 2827–2831

Yang, J. T. & Samejima, T. (1969) *Prog. Nucleic Acid Res.* **9**, 223–300